Acta Crystallographica Section E
Structure Reports Online
ISSN 1600-5368

$(Ga_{0.71}B_{0.29})PO_4$ with a high-cristobalite-type structure refined from powder data

Ya-Xi Huang,[a]* Jin-You Liu,[a] Jin-Xiao Mi[a] and Jing-Tai Zhao[b]

[a]Department of Materials Science and Engineering, College of Materials, Xiamen University, Xiamen 361005, People's Republic of China, and [b]Chinese Academy of Sciences, Shanghai Institute of Ceramics, State Key Laboratory of High Performance Ceramics and Superfine Microstructure, 1295 Dingxi Road, Shanghai 200050, People's Republic of China
Correspondence e-mail: yaxihuang@xmu.edu.cn

Received 16 December 2009; accepted 5 January 2010

Key indicators: powder X-ray study; T = 293 K; mean σ(P–O) = 0.003 Å; disorder in main residue; R factor = 0.076; wR factor = 0.129.

Gallium boron phosphate, $(Ga_{0.71}B_{0.29})PO_4$, was synthesized by a high-temperature solid-state reaction method. The crystal structure is isostructural with the tetragonal high-cristobalite structure with space group $P\overline{4}$ which is built from alternating $Ga(B)O_4$ and PO_4 tetrahedra interconnected by sharing the common O-atom vertices, resulting in a three-dimensional structure with two-dimensional six-membered-ring tunnels running along the a and b axes.

Related literature

For information on cristobalite structures, see: Achary *et al.* (2003). For borophosphate structures, see: Ewald *et al.* (2007); Mi *et al.* (1999); Schmidt *et al.* (2004); Schulze (1934); Dachille & Glasser (1959); Mackenzie *et al.* (1959). For the catalytic properties of BPO_4, see: Moffat (1978); Moffat & Schmidtmeyer (1986); Mooney (1956); Morey *et al.* (1983); Tada *et al.* (1987); Tartarelli *et al.* (1970). For crystallographic background, see: Finger *et al.* (1994)); Thompson *et al.* (1987).

Experimental

Crystal data

$(Ga_{0.71}B_{0.29})PO_4$
M_r = 147.61
Tetragonal, $P\overline{4}$
a = 4.7343 (1) Å
c = 7.0896 (4) Å
V = 158.90 (1) Å^3
Z = 2
Cu $K\alpha_1$, Cu $K\alpha_2$ radiation
λ = 1.5405, 1.5443 Å
T = 293 K
flat sheet, 10 × 10 mm

Data collection

Rigaku-D/max automatic powder diffractometer
Specimen mounting: packed powder pellet
Data collection mode: reflection
Scan method: step
$2\theta_{min}$ = 15.03°, $2\theta_{max}$ = 100.02°, $2\theta_{step}$ = 0.01°

Refinement

R_p = 0.076
R_{wp} = 0.129
R_{exp} = 0.072
$R(F^2)$ = 0.07586
χ^2 = 3.204
8500 data points
35 parameters
2 restraints

Table 1
Selected bond lengths (Å).

(Ga/B)1—O2^{i}	1.7079 (5)	P1—O1	1.499 (3)
(Ga/B)2—O1^{ii}	1.6979 (5)		

Symmetry codes: (i) $x, y, z-1$; (ii) $x-1, y, z$.

Cell refinement: *GSAS* (Larson & Von Dreele, 2004); data reduction: *GSAS*; program(s) used to refine structure: *GSAS* (Larson & Von Dreele, 2004); molecular graphics: *DIAMOND* (Brandenburg, 2005); software used to prepare material for publication: *GSAS*.

This project was supported by the National Natural Science Foundation of China (No. 40972035) and State '973' project (No. 2007CB936704).

Supplementary data and figures for this paper are available from the IUCr electronic archives (Reference: BR2131).

References

Achary, S. N., Jayakumar, O. D., Tyagi, A. K. & Kulshreshtha, S. K. (2003). *J. Solid State Chem.* **176**, 37–46.
Brandenburg, K. (2005). *DIAMOND*. Crystal Impact GbR, Bonn, Germany.
Dachille, F. & Glasser, L. S. D. (1959). *Acta Cryst.* **12**, 820–821.
Ewald, B., Huang, Y.-X. & Kniep, R. (2007). *Z. Anorg. Allg. Chem.* **633**, 1517–1540.
Finger, L. W., Cox, D. E. & Jephcoat, A. P. (1994). *J. Appl. Cryst.* **27**, 892–900.
Larson, A. C. & Von Dreele, R. B. (2004). *General Structure Analysis System (GSAS)*. Report LAUR, 86-748. Los Alamos National Laboratory, New Mexico, USA.
Mackenzie, J. D., Roth, W. L. & Wentorf, R. H. (1959). *Acta Cryst.* **12**, 79.
Mi, J.-X., Mao, S.-Y., Chen, Z.-H., Huang, Z.-L. & Zhao, J.-T. (1999). *Chin. Chem. Lett.* **10**, 707–708.
Moffat, J. B. (1978). *Catal. Rev. Sci. Eng.* **18**, 199–258.
Moffat, J. B. & Schmidtmeyer, A. (1986). *Appl. Catal.* **28**, 161–168.
Mooney, R. C. L. (1956). *Acta Cryst.* **9**, 728–734.
Morey, J., Marinas, J. M. & Sinisterra, J. V. (1983). *React. Kinet. Catal. Lett.* **22**, 175–180.
Schmidt, M., Ewald, B., Prots, Yu., Cardoso-Gil, R., Armbrüster, M., Loa, I., Zhang, L., Huang, Y.-X., Schwarz, U. & Kniep, R. (2004). *Z. Anorg. Allg. Chem.* **630**, 655–662.
Schulze, G. E. R. (1934). *Z. Phys. Chem.* **24**, 215–240.
Stephens, P. W. (1999). *J. Appl. Cryst.* **32**, 281–289.
Tada, A., Suzuka, H. & Imizu, Y. (1987). *Chem. Lett.* **2**, 423–424.
Tartarelli, R., Giorgini, M., Lucchesi, A., Stoppato, G. & Moreli, F. (1970). *J. Catal.* **17**, 41–45.
Thompson, P., Cox, D. E. & Hastings, J. B. (1987). *J. Appl. Cryst.* **20**, 79–83.

supplementary materials

Acta Cryst. (2010). E**66**, i4 [**doi:10.1107/S1600536810000358**]

$(Ga_{0.71}B_{0.29})PO_4$ with a high-cristobalite-type structure refined from powder data

Y.-X. Huang, J.-Y. Liu, J.-X. Mi and J.-T. Zhao

Comment

The high-cristobalite boron phosphate has long been used as an effective catalyst for various organic reactions such as hydration, dehydration, oligomerization (Moffat, 1978; Moffat & Schmidtmeyer, 1986; Morey *et al.*, 1983; Tada *et al.*, 1987; Tartarelli *et al.*, 1970). The catalytic activities depend on the ratio of P/B and surface area. In the case of excess B content, BPO_4 catalysts consist predominately of Lewis acid sites, and show catalytic efficiencies for the dehydration. In contrast, in a region consisting of excess phosphorus P content, BPO_4 catalysts have more Brønsted acid sites and exhibit catalytic activities for hydration. Applying trivalent cations to partially substitute boron may vary the ratio of P/B and modify the catalytic property. The possibility of modifying the catalytic properties by varieties of P/B ratio and searching for new phases in the borophosphate system intrigue us to investigate systems containing larger trivalent metal cations. In our previous investigations, a series of compounds with boron partially substituted by transition metals, such as Mn, Fe, Co, Ni, and Cu, has been characterized with low cristobalite type structure (Mi *et al.*, 1999). When we applied a smaller trivalent element Ga to modify the BPO_4, the occupancy of Ga is more than 50%, while less than 50% for transition metal compounds (*M* = Mn, Fe, Co, Ni, and Cu). In consequence, the structure of $(Ga_{0.71}B_{0.29})PO_4$ are high-cristobalite structure instead of low-cristobalite type structure.

The crystal structure of $(Ga_{0.71}B_{0.29})PO_4$ is isostructural with the tetragonal high-cristobalite structure (Schulze, 1934; Schmidt *et al.*, 2004) with space group $P\overline{4}$ which is built from alternating (Ga, B)O_4 and PO_4 tetrahedra interconnected by sharing the common O-vertices, resulting in a three dimensional network with two dimensional 6-membered ring tunnels running along the *a*- and *b*-axis, respectively. Every TO_4 (T = Ga(B), P) tetrahedron connects to four neighboring TO_4 tetrahedra. There are three types of positions for T-atoms. (Ga, B)1 and (Ga, B)2 sit at 1*c* and 1*b*, while P at 2*g*. The long (Schläfli) notation for (Ga, B) nodes is $6_2.6_2.6_2.6_2.6_2.6_2$, while $6_2.6_2.6_2.6_2.6_2.6_2$ for the P nodes, giving the net symbol $(6_2.6_2.6_2.6_2.6_2.6_2)_3$ which can be represented by the short symbol $(6^6)_3$.

The (Ga, B)1–O and (Ga, B)2–O bond distances are 1.7079 (5) Å and 1.6979 (5) Å in the (Ga, B)O_4 tetrahedra which are significantly larger than the B–O bond value of 1.463 Å in BPO_4 (Schmidt *et al.*, 2004), but smaller than the bond values of 1.829 Å for Ga–O bond in $GaPO_4$ (Achary *et al.*, 2003), indicating that boron and gallium occupy the same position. After refining both the atomic occupation number and displacement parameters, it results in the ratio of Ga:B = 0.71:0.29. In turn, the Ga:P is 1.42:2, which is quite good agreement with that (Ga:P = 3:4) in the reactants for obtaining the pure phase. The introduction of gallium in the compound led to the deformation of all the tetrahedra and quite anisotropic expansion of the structure which results in lowering symmetry from space group $I\overline{4}$ of BPO_4 to $P\overline{4}$ for the new compound.

Experimental

The title compound has been synthesized *via* high temperature solid state reaction method and the structure refined from X-ray powder diffraction data. A mixture of H_3BO_3, $NH_4H_2PO_4$, and Ga_2O_3 with molar ratio of B:Ga:*P* = 12:3:4 was well ground and reacted first at 973 K for 4 h, then cooled down to room temperature and reground again, pressed into pellets and reacted at 1373 K for 8 h, at last shut down the furnace and cooled down to room temperature. The extra B_2O_3 in the products were washed out by hot water.

Refinement

The cell parameters were obtained by least-square fits of the powder diffractometer data using silicon (a = 5.4308 Å) as an internal standard. Although the powder pattern and cell parameters are quite different from BPO_4, the starting atomic positional parameters can still be derived from the prototype BPO_4 (Schmidt *et al.*, 2004). During the initial refinement, the unreasonable negative thermal parameters for the B position are indicative of partial substitutions by Ga. The boron position then were assumed to be occupied by two kinds of atoms and the occupacies were allowed to vary during the subsequent refinements. Because it is difficult to refine both the occupation numbers and atomic displacement parameters at the same time, a two-step process was applied to refine the occupancy numbers and atomic displacement parameters. At the begining, all the atomic displacement parameters were set to one value to refine the occupancy number, then fixed the occupany number to refine the displacement parameters. Both processes were performed alternately several times till reasonable values for both atomic occupancies and displacement parameters were obtained. Due to the individual refinement, the standard deviations given by the program are much too small to be a realistic estimate of the uncertainty.

Figures

Fig. 1. Experimental (points) and calculated (lines) X-ray diffraction patterns of $(Ga_{0.71}B_{0.29})PO_4$. The difference profile is given at the bottom. The Bragg positions are indicated by the vertical marker below the observed pattern.

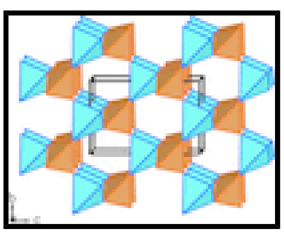

Fig. 2. The crystal structure of $(Ga_{0.71}B_{0.29})PO_4$ viewed along the a-axis. (Ga,B)O_4 tetrahedra: blue, PO_4 tetrahedra: orange.

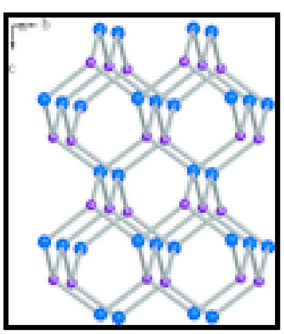

Fig. 3. Topological figure for the network of $(Ga_{0.71}B_{0.29})PO_4$, oxygen atoms were omitted for clarity. Ga(B) atoms: blue spheres, P atoms: purple spheres.

gallium boron phosphate

Crystal data

$(Ga_{0.71}B_{0.29})PO_4$	$Z = 2$
$M_r = 147.61$	$F(000) = 140.4$
Tetragonal, $P\overline{4}$	$D_x = 3.084$ Mg m^{-3}
Hall symbol: P -4	Cu $K\alpha_1$, Cu $K\alpha_2$ radiation, λ = 1.540500, 1.544300 Å
$a = 4.7343$ (1) Å	$T = 293$ K
$c = 7.0896$ (4) Å	white
$V = 158.90$ (1) Å^3	flat sheet, 10 × 10 mm

Data collection

Rigaku-D/max automatic powder diffractometer	Scan method: step
graphite	$2\theta_{min} = 15.03°$, $2\theta_{max} = 100.02°$, $2\theta_{step} = 0.01°$
Specimen mounting: packed powder pellet	DUMMY
Data collection mode: reflection	DUMMY

Refinement

Least-squares matrix: full	8500 data points
$R_p = 0.076$	Profile function: Thompson *et al.* (1987); Finger *et al.* (1994); Stephens et al. (1999)
$R_{wp} = 0.129$	35 parameters
$R_{exp} = 0.072$	2 restraints
$R(F^2) = 0.07586$	$(\Delta/\sigma)_{max} = 0.001$
$\chi^2 = 3.204$	Background function: The background function is a cosine Fourier series with a leading constant term. $I_b = B_1 + \Sigma B_j \cos[P^*(j-1)]$ (j=2-9), here P = 2θ, B_j (j = 1-9) values are given below: 1: 935.903 2: -1634.98 3: 1422.47 4: -1094.93 5: 681.394 6: -358.046 7: 116.953 8: -17.2104 9: -22.9558

Fractional atomic coordinates and isotropic or equivalent isotropic displacement parameters (Å^2)

	x	*y*	*z*	U_{iso}*/U_{eq}	Occ. (<1)
Ga1	0.5	0.5	0.0	0.0347 (12)*	0.7002 (4)
Ga2	0.0	0.0	0.5	0.0406 (11)*	0.7179 (3)
P1	0.5	0.0	0.7456 (5)	0.0447 (12)*	
O1	0.7299 (3)	0.1326 (3)	0.6304 (5)	0.0493 (15)*	
O2	0.6286 (3)	0.7718 (4)	0.8669 (5)	0.0511 (16)*	
B1	0.5	0.5	0.0	0.0347 (12)*	0.2998 (4)
B2	0.0	0.0	0.5	0.0406 (11)*	0.2821 (3)

Geometric parameters (Å, °)

(Ga/B)1—P1^{i}	2.9759 (8)	(Ga/B)2—O1^{ix}	1.6979 (5)
(Ga/B)1—P1^{ii}	2.9759 (8)	(Ga/B)2—O1^{x}	1.6979 (5)
(Ga/B)1—P1^{iii}	2.9759 (8)	P1—O1	1.499 (3)
(Ga/B)1—P1^{iv}	2.9759 (8)	P1—O1^{ix}	1.499 (3)
(Ga/B)1—O2^{i}	1.7079 (5)	P1—O2^{xi}	1.509 (3)
(Ga/B)1—O2^{iii}	1.7079 (5)	P1—O2^{xii}	1.509 (3)
(Ga/B)1—O2^{v}	1.7079 (5)	B1—O2^{i}	1.7079 (5)
(Ga/B)1—O2^{vi}	1.7079 (5)	B1—O2^{iii}	1.7079 (5)
(Ga/B)2—P1^{vii}	2.9386 (8)	B1—O2^{v}	1.7079 (5)
(Ga/B)2—P1	2.9386 (8)	B1—O2^{vi}	1.7079 (5)
(Ga/B)2—P1^{viii}	2.9386 (8)	B2—O1^{vii}	1.6979 (5)
(Ga/B)2—P1^{iii}	2.9386 (8)	B2—O1^{iii}	1.6979 (5)
(Ga/B)2—O1^{vii}	1.6979 (5)	B2—O1^{ix}	1.6979 (5)
(Ga/B)2—O1^{iii}	1.6979 (5)	B2—O1^{x}	1.6979 (5)
O2^{i}—(Ga/B)1—O2^{iii}	107.765 (2)	O2^{xi}—P1—O2^{xii}	110.502 (4)
O2^{i}—(Ga/B)1—O2^{v}	112.941 (3)	(Ga/B)2^{xiii}—O1—P1	133.541 (1)
O2^{i}—(Ga/B)1—O2^{vi}	107.765 (2)	P1—O1—B2^{xiii}	133.541 (1)
O2^{iii}—(Ga/B)1—O2^{v}	107.765 (2)	(Ga/B)1^{xiv}—O2—P1^{xv}	135.267 (1)
O2^{iii}—(Ga/B)1—O2^{vi}	112.941 (3)	P1^{xv}—O2—B1^{xiv}	135.267 (1)
O2^{v}—(Ga/B)1—O2^{vi}	107.765 (2)	O2^{i}—B1—O2^{iii}	107.765 (2)
O1^{vii}—(Ga/B)2—O1^{iii}	107.239 (2)	O2^{i}—B1—O2^{v}	112.941 (3)
O1^{vii}—(Ga/B)2—O1^{ix}	114.035 (3)	O2^{i}—B1—O2^{vi}	107.765 (2)
O1^{vii}—(Ga/B)2—O1^{x}	107.239 (2)	O2^{iii}—B1—O2^{v}	107.765 (2)
O1^{iii}—(Ga/B)2—O1^{ix}	107.239 (2)	O2^{iii}—B1—O2^{vi}	112.941 (3)
O1^{iii}—(Ga/B)2—O1^{x}	114.035 (3)	O2^{v}—B1—O2^{vi}	107.765 (2)
O1^{ix}—(Ga/B)2—O1^{x}	107.239 (2)	O1^{vii}—B2—O1^{iii}	107.239 (2)
O1—P1—O1^{ix}	113.942 (3)	O1^{vii}—B2—O1^{ix}	114.035 (3)
O1—P1—O2^{xi}	108.506 (2)	O1^{vii}—B2—O1^{x}	107.239 (2)
O1—P1—O2^{xii}	107.696 (2)	O1^{iii}—B2—O1^{ix}	107.239 (2)
O1^{ix}—P1—O2^{xi}	107.696 (2)	O1^{iii}—B2—O1^{x}	114.035 (3)
O1^{ix}—P1—O2^{xii}	108.506 (2)	O1^{ix}—B2—O1^{x}	107.239 (2)

Symmetry codes: (i) *x*, *y*, *z*−1; (ii) *x*, *y*+1, *z*−1; (iii) *y*, −*x*+1, −*z*+1; (iv) *y*+1, −*x*+1, −*z*+1; (v) −*x*+1, −*y*+1, *z*−1; (vi) −*y*+1, *x*, −*z*+1; (vii) *x*−1, *y*, *z*; (viii) *y*, −*x*, −*z*+1; (ix) −*x*+1, −*y*, *z*; (x) −*y*, *x*−1, −*z*+1; (xi) *x*, *y*−1, *z*; (xii) −*x*+1, −*y*+1, *z*; (xiii) *x*+1, *y*, *z*; (xiv) *x*, *y*, *z*+1; (xv) *x*, *y*+1, *z*.

Fig. 1

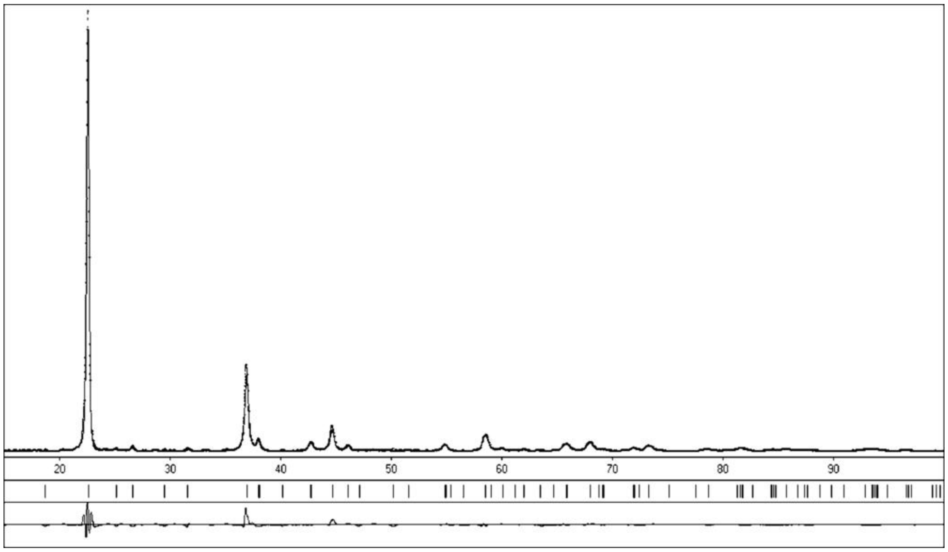

Fig. 2

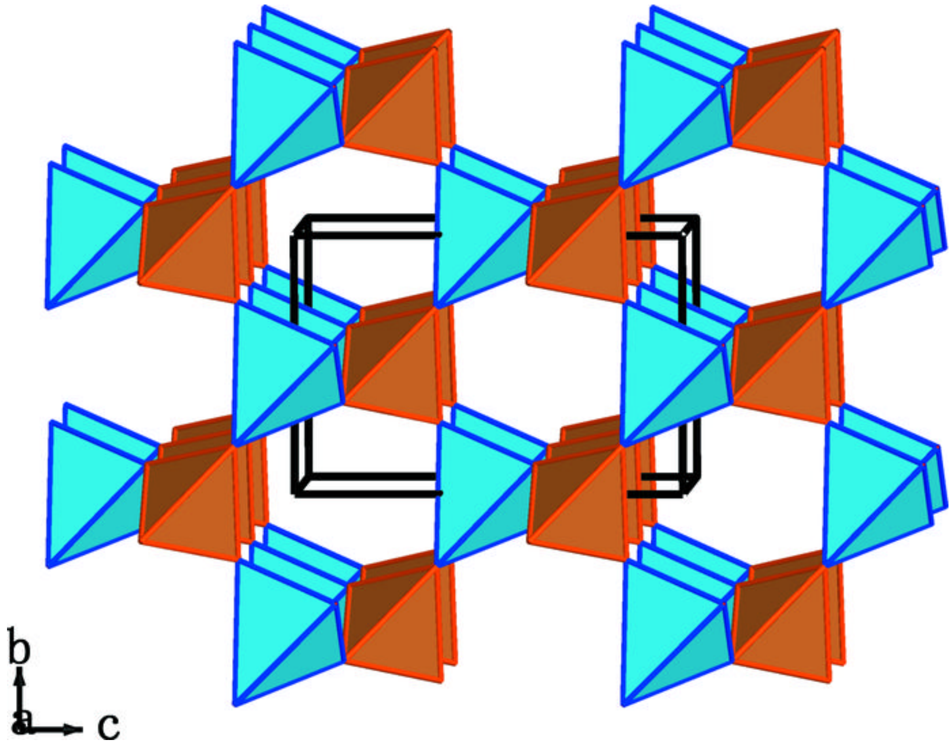

Fig. 3